OPEN

Intravascular Large B-Cell Lymphoma Genomic Profile Is Characterized by Alterations in Genes Regulating NF-κB and Immune Checkpoints

Blanca Gonzalez-Farre, MD, PhD,†‡ Joan E. Ramis-Zaldivar, PhD,†‡ Natalia Castrejón de Anta, MD,*† Alfredo Rivas-Delgado, MD,†§ Ferran Nadeu, PhD,†‡ Julia Salmeron-Villalobos, BS,†‡ Anna Enjuanes, PhD,† Kennosuke Karube, MD, PhD,‖ Olga Balagué, MD, PhD,*†‡ Francesc Cobo, MD, PhD,¶ Nicholas Kelleher, MD,# Ingrid Victoria, BS,* Luis Veloza, MD, PhD,*** Cristina Teixido, MD, PhD,*† Eva Giné, MD, PhD,†‡§ Mónica Lopez-Guerra, PhD,*†‡ Leticia Quintanilla-Martinez, MD, PhD,†† Armando Lopez-Guillermo, MD, PhD,†‡§ Itziar Salaverria, PhD,†‡ and Elias Campo, MD, PhD*†‡*

Abstract: Intravascular large B-cell lymphoma (IVLBCL) is an uncommon lymphoma with an aggressive clinical course characterized by selective growth of tumor cells within the vessels. Its pathogenesis is still uncertain and there is little information on the underlying genomic alterations. In this study, we performed a clinicopathologic and next-generation sequencing analysis of 15 cases of IVLBCL using a custom panel for the detection of alterations in 68 recurrently mutated genes in B-cell lymphomagenesis. Six patients had evidence of hemophagocytic syndrome. Four patients presented concomitantly a solid malignancy. Tumor cells outside the vessels were observed in 7 cases, 2 with an overt diffuse large B-cell cell lymphoma. In 4 samples, tumor cells infiltrated lymphatic vessel in addition to blood capillaries. Programmed death-ligand 1 (PD-L1) was positive in tumor cells in 4 of 11 evaluable samples and in macrophages intermingled with tumor cells in 8. *PD-L1* copy number gains were identified in a higher proportion of cases expressing PD-L1 than in negative tumors. The most frequently mutated gene was *PIM1* (9/15, 60%), followed by $MYD88^{L265P}$ and *CD79B* (8/15, 53% each). In 6 cases, $MYD88^{L265P}$ and *CD79B* mutations were detected concomitantly. We also identified recurrent mutations in *IRF4*, *TMEM30A*, *BTG2*, and *ETV6* loci (4/15, 27% each) and novel driver mutations in *NOTCH2*, *CCND3*, and *GNA13*, and an

From the *Pathology Department, Hospital Clínic de Barcelona, University of Barcelona; †Institut d'Investigacions Biomèdiques August Pi i Sunyer (IDIBAPS); §Hematology Department, Hospital Clinic de Barcelona, University of Barcelona, Barcelona; ‡Centro de Investigación Biomédica en Red de Cáncer (CIBERONC), Madrid; #Hematology Department, Hospital Universitari Josep Trueta, Girona, Spain; ‖Department of Pathology and Laboratory Medicine, Nagoya University Hospital, Nagoya, Japan; ¶Hematology Department, Hospital Nostra Senyora de Meritxell, Les Escaldes, Andorra; **Institute of Pathology, Lausanne University Hospital, Lausanne University, Lausanne, Switzerland; and ††Institute of Pathology and Neuropathology and Comprehensive Cancer Center Tübingen, University Hospital Tübingen, Eberhard-Karls-University, Tübingen, Germany.

B.G.-F., J.E.R.-Z., I.S., and E.C. contributed equally.

This study was approved by the Institutional Review Board of Hospital Clínic Barcelona. Informed consent was obtained from all patients in accordance with the Declaration of Helsinki.

B.G.-F. performed morphologic diagnosis, analyzed data, and wrote the manuscript. J.E.R.-Z. performed research, analyzed data, and wrote the manuscript. N.C., A.R.-D., F.N., J.S.-V., A.E., M.L.-G. performed research and analyzed data. K.K., O.B., F.C., N.K., I.V., L.V., C.T., E.G., L. Q.-M., A.L.-G. reviewed and interpreted pathologic and/or clinical data. I.S. performed research, analyzed data, designed research, and wrote the manuscript. E.C. performed morphologic analysis, designed research, and wrote the manuscript.

Conflicts of Interest and Source of Funding: Supported by the Ministerio de Ciencia e Innovación (MCI), Grant No. PID2021-123054OB-I00 (to E.C.), the European Regional Development Fund "Una manera de fer Europa" and Generalitat de Catalunya Suport Grups de Recerca (2017-SGR-1142 E.C.). J.E.R.-Z. was supported by a fellowship from Generalitat de Catalunya AGAUR FI-DGR 2017 (2017 FI_B01004). I.S. is a Miguel Servet II researcher from Instituto de Salud Carlos III (MS18/0015). E.C. is an Academia Researcher of the "Institució Catalana de Recerca i Estudis Avançats" (ICREA) of the Generalitat de Catalunya. This work was developed at the Centro Esther Koplowitz, Barcelona, Spain. The group is supported by Acció instrumental d'Incorporació de Científics i Tecnòlegs PERIS 2016 and 2020 (SLT002/16/00336 and SL017/20/000204 to N.G.) from Generalitat de Catalunya. The authors have disclosed that they have no significant relationships with, or financial interest in, any commercial companies pertaining to this article.

Correspondence: Elias Campo, MD, PhD, Department of Anatomic Pathology, Hospital Clinic of Barcelona, Calle Villarroel 170, 08036 Barcelona, Spain (e-mail: ecampo@clinic.cat).

Supplemental Digital Content is available for this article. Direct URL citations appear in the printed text and are provided in the HTML and PDF versions of this article on the journal's website, www.ajsp.com.

IRF4 translocation in 1 case each. The mutational profile was similar in patients with and without evidence of hemophagocytic syndrome and in cases with or without dissemination of tumor cells outside the vessels. Our results confirm the relevance of mutations in B-cell receptor/nuclear factor-κB signaling and immune escape pathways in IVLBCL and identify novel driver alterations. The similar mutational profile in tumors with extravascular dissemination suggests that these cases may also be considered in the spectrum of IVLBCL.

Key Words: intravascular lymphoma, PD-L1, NF-κB, NHL

(*Am J Surg Pathol* 2023;47:202–211)

Intravascular large B-cell lymphoma (IVLBCL) is a rare type of extranodal large B-cell lymphoma characterized by the selective growth of lymphoma cells within the lumen of capillaries and small vessels. Although the pathogenic mechanisms determining this tropism are not well understood, IVLBCL has been related to alterations in adhesion molecules and chemokines regulating interactions between tumor and endothelial cells and tumor cell motility.[1–3] The particular growth of this neoplasia makes the clinical manifestations extremely variable and most of the signs and symptoms are related to the preferentially involved organs. The absence of remarkable lymphadenopathy, and the nonspecific clinical symptoms such as fever of unknown origin and general malaise, makes precise diagnosis difficult. This, results in a delay of the diagnosis, disease progression, and poor prognosis.[3] Although in the past most cases were identified at autopsy,[4] nowadays the diagnosis is made during the clinical course in ∼80% of patients.[5–7] The clinical presentation is heterogeneous and 3 major variants are recognized, namely classic, hemophagocytic syndrome (HPS)-associated form, and isolated cutaneous. This later clinical subtype has been associated with a better prognosis.[3,8]

Recent studies are starting to elucidate the genetic and molecular alterations involved in the pathogenesis of this tumor. Conventional cytogenetic studies and copy number (CN) arrays of patients-derived xenografts have identified complex karyotypes with recurrent cytogenetic abnormalities involving chromosomes 1, 6q, 8p, 9p, 18, 19q, and some samples with tetraploidy.[9–11] Genetic-targeted next-generation sequencing (NGS) studies in small series of IVLBCL have revealed high prevalence of *MYD88* and *CD79B* mutations.[12,13] More recently, Shimada et al[14] performed a comprehensive genetic analysis of mainly cell-free DNA specimens of 21 IVLBCL by whole-exome sequencing identifying high frequency of genetic alterations characteristic of activated B-cell diffuse large B-cell lymphoma (DLBCL) or central nervous system (CNS) lymphomas, related with evasion of immune checkpoint. These alterations included mutations in B-cell receptor (BCR)/nuclear factor-κB (NF-κB) signaling pathways in addition to *CDKN2A/2B* deletions and structural variants and CN gains involving *PD-L1*.[14] In addition, a recent whole-exome sequencing analysis in autopsy cases have identified *RAC2* mutations, downstream of BCR activation, in 4 of the 6 investigated cases.[15] All the mutational studies of IVLBCL on tissue specimens have been restricted to the analysis of short series of cases or by means of custom NGS panels interrogating a limited number of genes. Moreover, these studies have not analyzed the relationship between the mutational profile and clinical or pathologic features of the patients. Therefore, the present study aims to expand the knowledge of the genomic alterations of IVLBCL and define their association with clinical and pathologic features of this unusual entity.

MATERIALS AND METHODS

Patients and Samples

A total of 15 patients diagnosed with IVLBCL according to the 2017 World Health Organization Classification[3] with available formalin-fixed paraffin-embedded tissue samples were included. All cases corresponded to the classic or the HPS form since no cases of the isolated cutaneous variant were available. IVLBCL diagnosis was established at autopsy in 7 patients (47%), surgical specimens in 5 (33%), and excisional biopsies in 3 (20%) (Table 1). The main clinicobiological characteristics were collected. Patients who had histologic evidence of hemophagocytosis and/or met the HLH-2004 diagnostic criteria for secondary hemophagocytic lymphohistiocytosis based on available retrospective data, were classified as HPS variant.[16,17]

Immunohistochemistry

Immunohistochemical studies were carried out with a panel of monoclonal and polyclonal antibodies reactive in formalin-fixed paraffin-embedded tissue sections using a peroxidase-labeled detection system, standard antigen retrieval protocols, and an automated immunostainer (Dako OMNIS; Dako or BenchmarkXT; Roche Diagnostics with ultraView or optiview Universal DAB Detection Kit). The panel of antibodies included common B-cell and T-cell markers as well as IRF4/MUM1, CD31, podoplanin, and PD-L1 (22C3) (Supplementary Table 1, Supplemental Digital Content 1, http://links.lww.com/PAS/B441). According to previous studies, MYC was considered positive when >40% of positive tumor cells were observed.[18] BCL6, CD10, and IRF4/MUM1 were considered positive if 30% or more of the tumor cells were stained with the antibody.[19] Following the criteria of previous publications, tumors were considered PD-L1 positive when >10% of tumor cells showed membrane staining.[20,21]

In Situ Hybridization

Epstein-Barr virus (EBV) was studied by in situ hybridization using EBV-encoded small RNA (EBER1, 2) probes (Leica BOND-MAX system; Leica Biosystems). Genetic alterations of *IRF4* were analyzed using home-made break-apart fluorescence in situ hybridization (FISH) probe as previously described.[22] In detail, the

design was 5′ IRF4 BAC clone RP3-416J7 labeled in Spectrum red and 3′ IRF4 BAC clones RP5-1077H22 and RP5-856G1 labeled in Spectrum green. IGH, IGK, and IGL breaks were analyzed in case #17 using IGH, IGK, and IGL XL break-apart FISH probes (Metaystems). FISH analysis for the identification of gains of *PD-L1* was performed using *PD-L1* locus-specific probes (Agilent) as previously described.[23] The tumor areas to be evaluated were identified by overlapping the FISH slides with the previously marked CD20 immunohistochemical stain and by unequivocally detecting the presence of vascular lumens. One hundred intact, nonoverlapping nuclei of intraluminal cells were analyzed in representative areas. Cells with 2 copies of each probe were defined as disomic, and those with a ratio of 1 but >2 copies of each probe were defined as polysomic. Those cells with a ratio of >1:1 but <3:1 were classified as having *PD-L1* copy gain, and those with a ratio of ≥3:1 were classified as being amplified for *PD-L1*, as previously defined.[24] A case was classified as presenting *PD-L1* CN alterations (CNAs) when the total number of CNAs (*PD-L1* polysomies, gains, amplifications) were >10%.

Mutational Analysis

The mutational status of all cases was studied with a panel of 68 B-cell lymphoma–related genes (Supplementary Table 2, Supplemental Digital Content 2, http://links.lww.com/PAS/B442) using a SureSelectXT Target Enrichment System Capture NGS strategy library (Agilent Technologies) before sequencing in a MiSeq equipment (Illumina). The average sequencing coverage of the 15 cases across regions was 516× (range: 121 to 989×) and over 94% of the targeted regions were covered by at least 100 reads. Variant calling was performed using 6 different

TABLE 1. Main Baseline Features, Treatment, and Response of the 15 Patients With IVLBCL

Case #	Sex/ age	Ethnicity	Sample	Involvement at diagnosis	Ann Arbor stage	B symptoms	LDH	IPI	HPS	Other neoplasia	Treatment	Response to treatment	Status at last follow-up
#1	M/ 83	Caucasian	Autopsy	Liver, GI tract, testicular, kidney, spleen, pancreas, lung, prostate	IV	No	Elevated	5	No	No	No	—	DOD
#2	F/54	Caucasian	Autopsy	Omentum, uterus, ovaries, lung, GI tract, periadrenal fat	IV	Yes	Elevated	3	Yes	No	No	—	DOC
#3	F/68	NA	Surgical specimen	Uterus	I	NA	NA	NA	NA	NA	NA	NA	NA
#5	F/80	Caucasian	Autopsy	CNS, adrenal glands and abdominal lymph nodes	IV	NA	NA	NA	NA	DLBCL	No	—	DOD
#9	M/ 75	Caucasian	Surgical specimen	Kidney	I	No	Elevated	2	No	Renal cell carcinoma	R-CHOP	CR	21 mo NED
#10	M/ 76	Caucasian	Surgical specimen	Prostate	I	NA	NA	NA	NA	NA	NA	NA	NA
#11	F/59	Caucasian	Autopsy	Widespread disease	IV	NA	NA	NA	NA	No	No	—	DOD
#12	M/ 64	Caucasian	Autopsy	Testicular, kidney, adrenal, bladder, prostate, liver, spleen, pancreas, GI tract, lung, heart, CNS	IV	NA	Elevated	5	NA	Lung adenocarcinoma	No	—	DOD
#13	F/81	Asian	Autopsy	Widespread disease	IV	Yes	Elevated	5	Yes	No	Steroids	No	DOD
#14	M/ 46	Caucasian	Surgical specimen	CNS, liver, lung, bone, penis	IV	Yes	Elevated	4	Yes	Penile squamous carcinoma	R-CHOP	CR	39 mo NED
#15	F/84	Caucasian	Autopsy	CNS, lung, GI tract	IV	Yes	Elevated	5	Yes	Lung neuroendocrine carcinoma	No	—	DOD
#16	F/60	Caucasian	Biopsy	CNS	I	No	Elevated	2	No	No	R-CHOP	PD	0.9 mo DOD
#17	F/59	Caucasian	Biopsy	Bone marrow	IV	Yes	Elevated	2	Yes	No	R-CHOP	CR	27 mo NED
#18	M/ 71	Caucasian	Surgical specimen	Prostate, liver, adrenal glands	IV	Yes	Elevated	5	No	No	R-CHOP	CR	26 mo NED
#21	M/ 59	Caucasian	Biopsy	Liver and bone marrow	IV	Yes	Elevated	4	Yes	No	R-CHOP	NE	1 mo DOC

CR indicates complete response; DOC, died of complications; DOD, died of disease; F, female; GI, gastrointestinal; IPI, International Prognostic Index; LDH, lactate dehydrogenase; M, male; NA, not available; NE, not evaluable; NED, alive, no evidence of disease; PD, progression disease; R-CHOP, rituximab, cyclophosphamide, doxorubicin, vincristine, and prednisone.

variant callers, as previously described.[25] For each variant caller, low-quality variants were excluded using default thresholds and only those variants identified by >2 algorithms were considered. Bioinformatic pipeline included a filtering process to exclude intronic, synonymous, and single-nucleotide polymorphism variants, and to select driver mutations with potential functional effect (Supplementary Methods, Supplemental Digital Content 3, http://links.lww.com/PAS/B443).

Statistical Analyses

R software (3.6.2 version) was used for statistical analyses. Differences in the distribution of individual parameters among patient subsets were analyzed by Fisher exact test for categorical variables, and the Student *t* test for continuous variables. Nonparametric tests were applied when necessary. *P* values for multiple comparisons were adjusted using the Benjamini-Hochberg correction (false discovery rate). A cutoff of $P = 0.05$ was considered significant unless otherwise indicated.

RESULTS

Clinical Features

The main clinicobiological features of the series are listed in Table 1. The median age of the patients was 68 years (range: 46 to 83 y). All patients were Caucasian except 1 from Asian origin. All showed high lactate dehydrogenase levels, 73% of patients had advanced stage (Ann Arbor stage IV), and the majority (73%) showed high-intermediate or high-risk IPI. Ten patients presented with >1 organ involved by IVLBCL. The tumor was histologically confirmed in multiple organs in all 7 autopsy cases and in case #21. In cases #14 and #18 we confirmed histologically the involvement of liver and penis and prostate, respectively. Analytical or image findings suggested the presence of the tumors in other sites (Table 1). Of note, 40% of patients presented CNS involvement. Six fulfill the criteria for HPS variant. Synchronous solid malignancies were diagnosed in 4 cases (renal cell carcinoma, penile squamous cell carcinoma, lung adenocarcinoma, and neuroendocrine carcinoma of the lung) (Fig. 1). In those 4 cases, the IVLBCL was initially diagnosed in the intratumoral vessels of these neoplasms.

Six patients were treated with R-CHOP (rituximab, cyclophosphamide, doxorubicin, vincristine, and prednisone). After frontline treatment, 4 (67%) patients achieved a complete response, and 2 (33%) were refractory, including 1 early decease. None of the 4 patients who achieved a complete response relapsed during the follow-up (Table 1).

Pathologic Features and FISH Analysis

All specimens showed characteristic features with the presence of atypical lymphoid cells within the lumen of blood capillaries and small vessels (Figs. 1, 2; Supplementary Fig. 1, Supplemental Digital Content 4, http://links.lww.com/PAS/B444). Sinusoidal involvement was detected in the liver and bone marrow of the analyzed samples. Interestingly, tumor cells inside lymphatic vessels, highlighted with podoplanin stain, were also detected in 4 cases (Fig. 2, Table 2). Extravascular spread of neoplastic lymphoid cells was seen in 7 patients in different proportions. In 3 patients, only isolated single cells or small clusters were detected. In 2 samples the tumor cells formed small sheets of at least 2mm in the vicinity of the vessels (Fig. 2, Table 2; Supplementary Fig. 2, Supplemental Digital Content 5, http://links.lww.com/PAS/B445). The remaining 2 patients had an overt lymphoma. One of those (#5) had an exclusive intravascular involvement in the brain and an overt DLBCL in the adrenal gland and abdominal lymph nodes. The same clonal IGH rearranged peak was demonstrated in both intravascular component and tumoral areas. The other case (#13) had the full spectrum of features with exclusive intravascular involvement in lungs, liver, bone marrow, and urinary tract, sheets of tumor cells outside the vessels in the small intestine, and an overt lymphoma in the adrenal gland. Unfortunately, clonality studies, in this case were not successful probably due to the DNA quality of the autopsy. Three of the 4 cases in which the IVLBCL was diagnosed in the intratumor vessels of a solid tumor had also a widespread disease with IVLBCL involvement demonstrated in at least 3 different organs (Table 1).

The atypical cells were consistently positive for CD79a in all cases and CD20 in 14 of the 15. Eight cases coexpressed CD5 in the neoplastic cells and, as expected, most tumors (13/15) showed an activated B-cell phenotype according to the Hans' algorithm (Table 2). MUM1/IRF4 was positive in 11 of 13 cases evaluable. Two cases expressed CD10. All samples were EBV (EBV-encoded small RNA) negative. PD-L1 stain was positive in 4 of the 11 evaluable cases (36%) showing uniform membrane expression in >10% of tumor cells. Macrophages intermingled with tumor cells inside the vessels were identified in 11 samples, 8 of them showing positivity for PD-L1 (Supplementary Fig. 1, Supplemental Digital Content 4, http://links.lww.com/PAS/B444, Table 2). Significant *PD-L1* CN gains and amplifications (>10% of tumor cells) were identified in 3/9 (33%) in a variable percentage of cells (Table 2, Supplementary Table 3, Supplemental Digital Content 6, http://links.lww.com/PAS/B446). *IRF4* rearrangement was detected in 1 of 11 specimens investigated expressing IRF4/MUM1 (Fig. 2).

Mutational Landscape of IVLBCL

The NGS performed in the 15 IVLBCL identified 141 mutations (Supplementary Table 4, Supplemental Digital Content 7, http://links.lww.com/PAS/B447). A total of 107 variants were predicted as potential driver mutations with a mean of 7.1 driver mutations per case (range: 1 to 15). The most recurrently mutated genes were *PIM1* (9/15, 60%), *MYD88*, and *CD79B* (8/15, 53% each) followed by *IRF4*, *TMEM30A*, *BTG2*, and *ETV6* found in 4 cases each (27% each) (Fig. 3). All *MYD88* mutations identified occurred in the hotspot p.L265P, whereas all *CD79B* mutations were in the ITAM domain (amino acids 193-210) affecting the hotspot in the amino acid Y197 except for 2 mutations in p.Y121AD and p.S42C. Interestingly, *MYD88* or *CD79B* mutations were present in 10 cases (67%) and cooccurred in 6 (40%) of them. All *IRF4* mutations in the 4 cases occurred in the 5′ region of

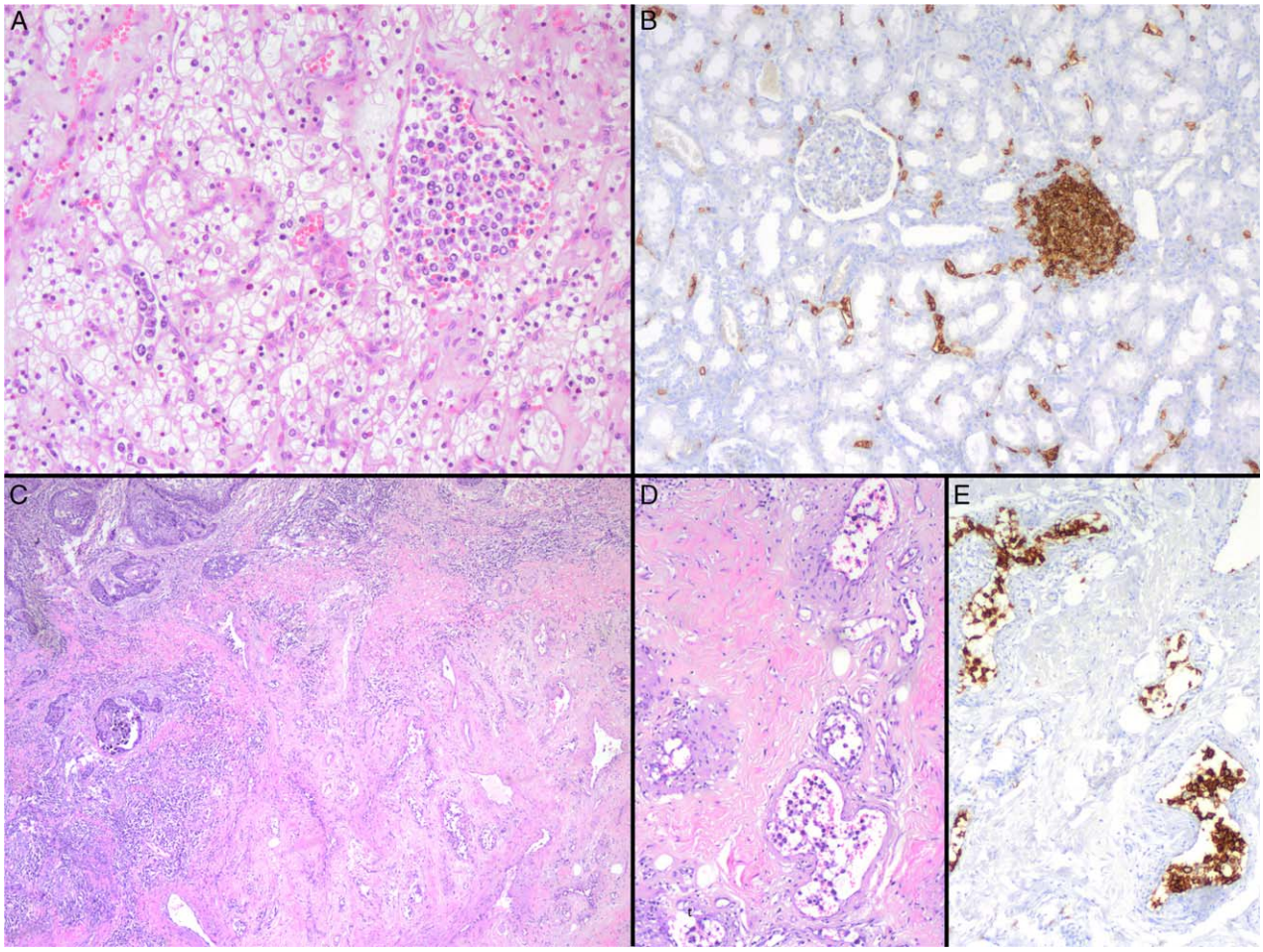

FIGURE 1. Morphologic and immunophenotypic features of 2 cases with synchronous occurrence of IVLBCL and malignant tumors (cases #9 and #14). A, Large and atypical lymphoid cells within vascular structures of a clear cell renal cell carcinoma (case #9, hematoxylin and eosin). B, CD20-positive neoplastic cells within small vessels in nontumoral renal parenchyma of the same case. An aggregate of B-cell nontumoral lymphocytes is also seen in the right site of the image (case #9, CD20 immunostain). C, Atypical lymphoid cells within the lumen of vascular spaces identified at the infiltrating border of a penile squamous cell carcinoma and also involving vessels of the adjacent nontumoral parenchyma (case #14, hematoxylin and eosin). D, Numerous atypical lymphocytes inside vascular structures at the surrounding parenchyma of the penile squamous cell carcinoma (case #14, hematoxylin and eosin). E, Tumoral cells show an intense positivity for CD20 (case #14, CD20 immunostain).

the gene. Two cases had multiple mutations (>2 mutations/case including passenger mutations) and in one of them (#3) we could demonstrate a concurrent *IRF4* rearrangement, as previously described in LBCL cases with *IRF4* translocations but not in IVLBCL (Supplementary Fig. 3, Supplemental Digital Content 8, http://links.lww.com/PAS/B448).[26,27] In case #17 with *IRF4* mutations but not identified *IRF4* translocation, we studied the presence of IGH, IGK or IGL breaks that would suggest the presence of a cryptic *IRF4* translocation with an IG partner, but all 3 loci were negative for rearrangements. The 4 mutations in *TMEM30A* were truncating as described previously in DLBCL.[28] Other novel genes with mutations involving known functional domains and predicted as drivers were *NOTCH2* with a truncating mutation in the PEST domain, *CCND3* with p.I290K, and *GNA13* with p.I366T mutations, observed in 1 case each. Pathway enrichment analysis (Supplementary Table 2, Supplemental Digital Content 2, http://links.lww.com/PAS/B442) showed NF-κB (87%), epigenetic modifiers (47%), immune response (33%), and B-cell differentiation (27%) as the most affected pathways.

No differences in individual mutated genes or pathways were observed in patients with or without evidence of HPS (Fig. 3). In detail, 4 of the 6 patients with evidence of HPS and 3 of 4 cases without HPS had mutations in *MYD88* and/or *CD79B*. Similarly, cases with tumor cells outside involved vessels had an analogous mutational profile than cases with only tumor cells inside the vessels. Four of the 7 cases with tumor cells outside the vessels had mutations in *MYD88* and/or *CD79B* and 4 had *PIM1* mutations. Similarly, *MYD88*/*CD79B* and

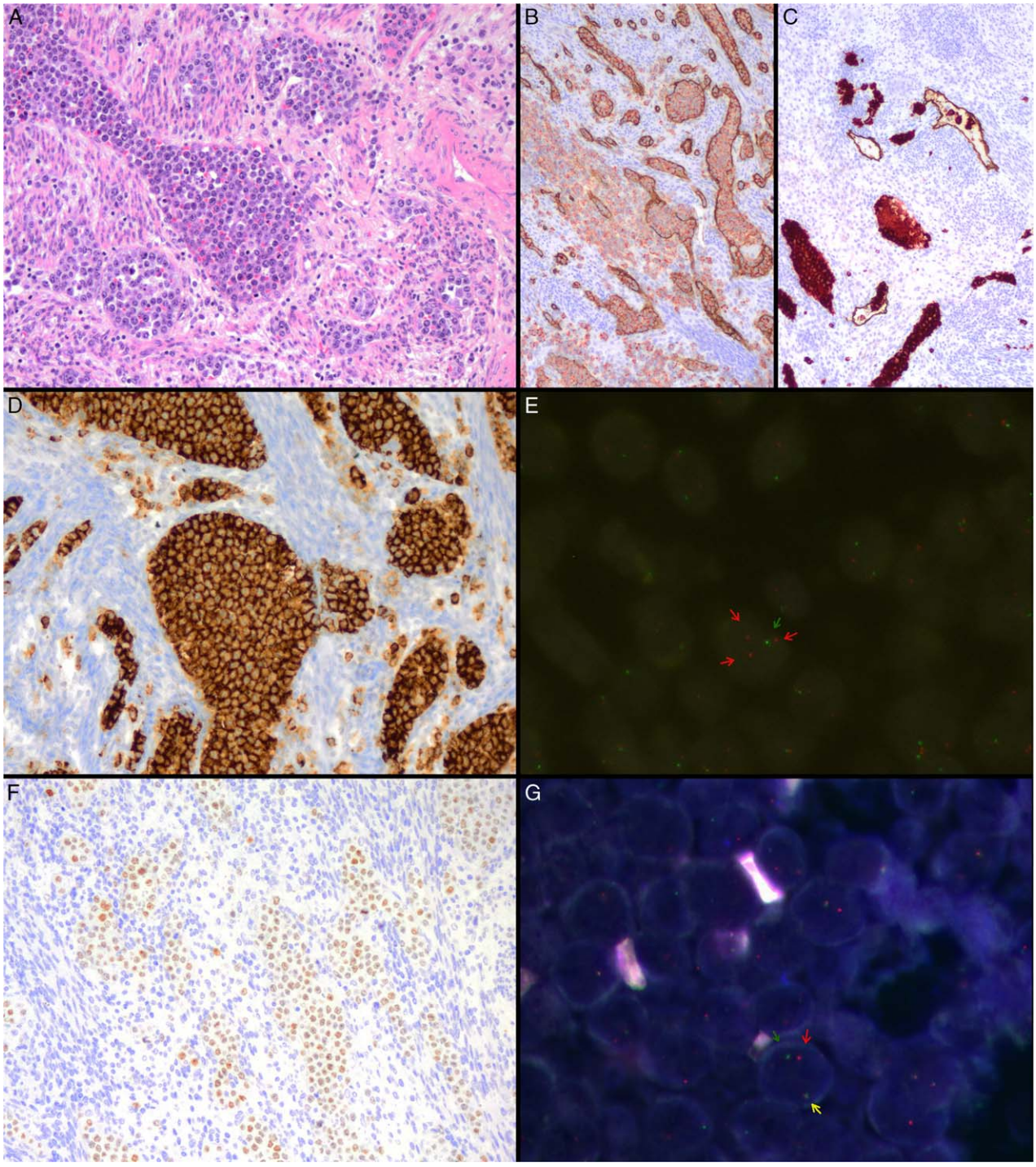

FIGURE 2. Morphologic and immunophenotypic features of IVLBCL with extravascular invasion (case #3). A, Numerous large and atypical lymphocytes within vascular channels and extravascular spread to the adjacent myometrium (hematoxylin and eosin). B, CD20-positive tumoral cells stained in red color are identified both within blood vessels and in the nearby parenchyma (Double immunostain for CD20 in red and CD34 in brown). C, CD20-positive tumoral cells stained in red color are also identified in lymphatic vessels (in the lower part of the image) and in the extravascular compartment of the adjacent parenchyma (in the upper part of the image) (Double immunostain for CD20 in red and podoplanin in brown). D, Neoplastic cells show an intense and diffuse positivity for PD-L1 (Immunostain). E, FISH analysis for *PD-L1* gene using locus-specific probes demonstrates > 2 red signals in each nucleus consisting with gains of the gene. Green signals correspond to the centromere used as a control (FISH for *PD-L1* gene to identify gains). F, Atypical cells show diffuse positivity for MUM1 (Immunostain). G, Break-Apart Probe (BAP) FISH for *IRF4* gene shows 1 colocalization signal and a pair of separated green and red signals in each nucleus consistent with the gene rearrangement (BAP FISH for *IRF4* gene).

TABLE 2. Morphologic, Immunohistochemical, and FISH Information of 15 IVLBCL

	Morphologic features		Immunohistochemistry										FISH	
Case #	Tumoral cells outside vessels*	Lymphatic involvement	CD20	CD79a	CD10	BCL6	MUM1	BCL2	CD5	CD30	PD-L1 tumor	PD-L1 histiocytes	*IRF4* BAP	PD-L1
#1	No	No	+	+	−	−	−	+	−	−	NA	NA	NA	−
#2	++	No	+	NA	−	−	+	+	+	−	−	+	Negative	−
#3	++	Yes	+	+	−	−	+	+	+	NA	100%	−	Positive	Amplification
#5	+++	Yes	+	+	+	−	NA	−	−	NA	NA	NA	Negative	−
#9	+	Yes	+	+	−	−	+	+	+	−	5%	+	Negative	−
#10	No	No	−	+	−	−	+	−	NA	−	70%	+	Negative	Amplification
#11	No	Yes	+	+	−	−	−	+	+	−	80%	+	Negative	NA
#12	+	No	+	+	−	+	+	+	+	−	−	+	Negative	−
#13	+++	NA	+	NA	−	−	NA	NA	+	−	NA	NA	NA	NA
#14	+	No	+	+	−	−	+	+	−	−	100%	+	Negative	Amplification
#15	No	No	+	+	−	−	+	+	−	−	−	+	NA	−
#16	No	No	+	+	−	+	+	+	+	−	−	−	Negative	NA
#17	No	No	+	NA	−	+	+	+	−	−	−	−	Negative	NA
#18	No	No	+	+	−	+	+	+	−	−	−	+	Negative	NA
#21	No	NA	+	NA	+	−	+	+	+	−	NA	NA	NA	NA

+ indicates immunostainings mean positive; −, negative staining; *, isolated or small clusters of tumor cells outside the vessels; ++, sheets of tumor cells outside the vessels; +++, areas of overt DLBCL; NA, not available.

PIM1 mutations were seen in 6 and 5 of the 8 cases with tumor cells exclusively seen inside the vessels, respectively (Fig. 3).

DISCUSSION

In the present study, we report a series of 15 IVLBCL in which we have observed unusual pathologic features such as lymphatic vessel involvement, extravascular spread, and co-occurrence with several types of solid neoplasms. Our findings confirm the high prevalence of mutations in genes involved the BCR/NF-κB signaling pathway and alterations in genes modulating the interactions of tumor cells with the microenvironment beyond the PD-L1 axis. We have also identified novel driver alterations in IVLBCL including an *IRF4* translocation and mutations of *NOTCH2*, *CCND3*, and *GNA13*.

The synchronous occurrence of IVLBCL and malignant tumors has been occasionally described in the literature.[29,30] In this context, the systemic clinical symptoms associated with the IVLBCL may mask the diagnosis of the solid neoplasm or vice versa. In our series, the diagnosis of IVLBCL was incidental during the surgical examination of a renal cell and a penile squamous cell carcinoma in cases #9 and #14, respectively. In the 2 remaining cases with the coexistence of lymphoid and epithelial tumors (#12 and #15), the diagnosis of the epithelial malignancy was obscured by the lymphoma involvement in many different organs. The association between IVLBCL and renal cell carcinoma and lung adenocarcinoma has been already described in the literature.[31,32] However, the coexistence with a penile squamous cell carcinoma (Figs. 1C–E) and lung neuroendocrine carcinoma has not previously reported.

The vessels involved by IVLBCL are classically described as blood microvessels. However, we could identify additional intralymphatic spread of neoplastic cells in 4 cases. This finding has been described in DLBCL as associated with poor prognosis,[33] but, as far as we know, has not been previously reported in IVLBCL. Minimal extravascular location of neoplastic B cells has been recognized in IVLBCL. However, if the tumor has a significant extravascular component the case has been better classified as DLBCL with vascular involvement.[3] Recently, Itami et al[34] showed that DLBCL with intravascular involvement behave more similar to IVLBCL than DLBCL from both clinical and pathologic points of view. In our cohort, we identified tumor cells infiltrating the tissues outside the vessels in 7 patients. Three samples presented just isolated single cells or small clusters outside the vessels, but in 2 cases sheets of neoplastic cells of at least 2 mm were identified and 2 patients had an overt DLBCL (Table 2, Supplementary Fig. 2, Supplemental Digital Content 5, http://links.lww.com/PAS/B445). The relative high proportion of cases in which we observed this feature may be because most of our IVLBCL were diagnosed either at autopsy or in surgical specimens in which we could study a large number of sections. The extensive intravascular involvement and the clinical presentation of these cases were like in those with pure intravascular involvement. In addition, the mutational profile was similar in cases with and without detected extravascular extension supporting that this may be a characteristic feature of IVLBCL. Patient #5 diagnosed at autopsy had extensive intravascular brain involvement and a tumor mass in the abdomen with the same clonal IGH rearrangement in both locations. Whether this case should be diagnosed as an IVLBCL with an associated DLBCL or a DLBCL with intravascular involvement may be debatable. The tumor carried *PIM1*, *CARD11*, and *BTG2* mutations that are common in both types of tumors but *MYD88* and *CD79B* were wild type.

The mutational landscape of our IVLBCL is concordant with a recent publication based on the analysis of

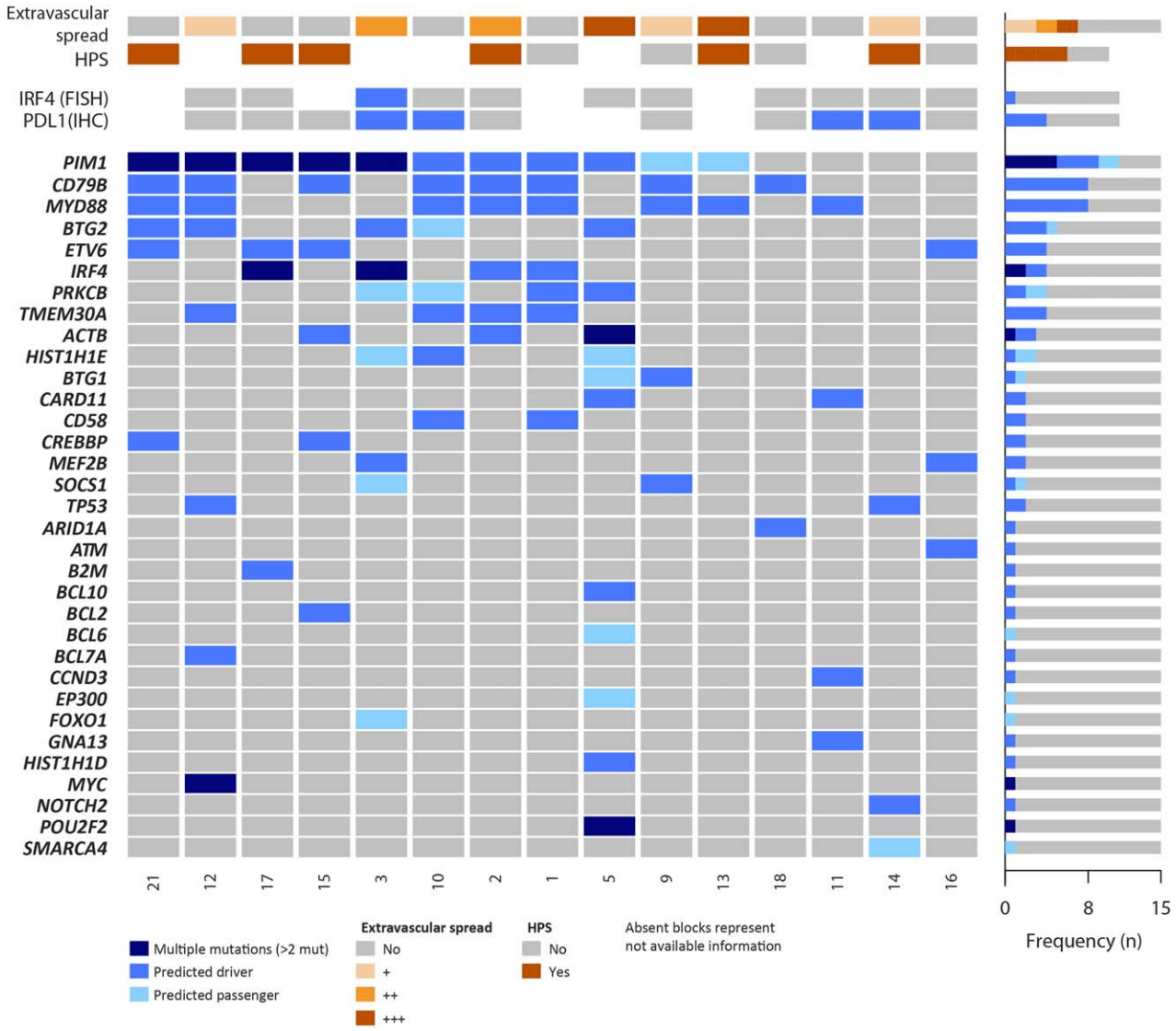

FIGURE 3. Mutational profile of 15 IVLBCL. Oncoprint including clinical and molecular features and recurrently mutated genes. Morphologic spectrum of extravascular spread are indicated as follows: (+) isolated or small clusters of tumor cells outside the vessels; (++) sheets of at least 2 mm of tumor cells outside the vessel, (+++) overt lymphoma.

circulating tumor DNA from patients with IVLBCL.[13,14] Our data confirm in a series of IVLBCL tissue biopsies that this disease also resembles genetically primary CNS lymphoma, primary testicular lymphoma, primary cutaneous DLBCL of leg-type, and a subgroup of mainly extranodal activated B-cell DLBCL. All these tumors have a genomic profile that correspond to that of the recently described genomic subgroup termed MCD or C5 (Supplementary Fig. 4A, Supplemental Digital Content 9, http://links.lww.com/PAS/B449).[35–37] The genomic similarities of all these tumors have raised the question whether they may correspond to the same biological category.[38] Although still, no major consensus exists on this idea, the fact that in our study tumors with and without extravascular dissemination, and even with an overt extranodal DLBCL, share the same mutational profile would support the concept that they may belong to the same biological entity, together with these other extranodal DLBCL. The different pathologic and clinical manifestations of the different subtypes could be due to additional particular molecular alterations in each entity.

The most recurrently mutated gene in our IVLBCL series was *PIM1* (60%), known target of somatic hypermutation (SHM). *PIM1* modulates NF-κB and JAK/STAT pathway and facilitates tumor immune escape in primary mediastinal B-cell lymphoma and classic Hodgkin lymphoma.[39,40] Other frequently mutated genes are involved in BCR/NF-κB signaling such as $MYD88^{L265P}$ and *CD79B* (53% each).[41,42] Interestingly, we also found truncating mutations in *TMEM30A* in a higher proportion (27%) of cases than in previous studies.[14,15] These mutations have been shown to increase BCR signaling in DLBCL, emphasizing the relevance of this

pathway in IVLBCL.[28] The recent identification of *RAC2* mutations in IVLBCL are concordant with these finding since this gene is activated on BCR stimulation and links BCR activation to cell adhesion.[15] We also observed *IRF4* mutations with a SHM pattern in a subset of IVLBCL (Supplementary Fig. 4B, Supplemental Digital Content 10, http://links.lww.com/PAS/B450),[14] Interestingly, we could identify an *IRF4* rearrangement in 1 of these cases (Fig. 2). The presence of *IRF4* SHM has been highly associated with *IRF4* translocation in other lymphomas.[26,27] Of note, Shimada and colleagues[14] found 4 IVLBCL carrying multiple mutations in *IRF4* although no specific information about whether these mutations had the SHM pattern was provided. Further analyses need to clarify whether *IRF4* translocations could be a recurrent aberration associated with the pathogenesis of IVLBCL. In addition to the *IRF4* translocation, we have identified novel driver alterations in *NOTCH2*, *CCND3*, and *GNA13*. The truncating *NOTCH2* mutation in the PEST domain stabilizes the protein and has been described in DLBCL, not otherwise specified.[37,43] Similarly, the *CCND3* mutation occurred in a hotspot that is recurrently mutated in DLBCL and Burkitt lymphoma leading to increased protein stability.[44] The *GNA13* mutation was predicted as driver and it is annotated as recurrent in several tumors in the COSMIC database.

The frequency of PD-L1 expression in our IVLBCL series (36%) is in line with the reported rates of 42% and 44% in 3 previous studies of IVLBCL.[14,45,46] Published data suggest that PD-L1 is expressed in both the so-called classic form as well as the HPS variant. Recently, Suzuki and colleagues reported a frequency of PD-L1 expression of 35% in a series of 34 Asian patients (using a cutoff value of 30%). Most of the positive samples of this series (9/12) corresponded to the HPS form. Remarkably, in that study PD-L1 expression was associated with younger age and worse survival among patients treated with multiagent chemotherapy that included rituximab compared with PD-L1 negative.[47] Our 2 patients with positive tumors and available clinical information (#11 and #14) also probably corresponded to the HPS variant. *PD-L1* genetic alterations including *PD-L1* CNAs have not been thoroughly studied in IVLBCL so far. In a recent study, Shimada and colleagues[14] identified recurrent structural variants and CN gains affecting *PD-L1*/*PD-L2* in 10 of 21 cases (48%). Also, Patel et al[46] identified chromosomal alterations in 7 of 29 cases (24%) including gains, amplifications, and rearrangements. Moreover, in both studies, PD-L1 overexpression was correlated with the presence of *PD-L1* involving genetic lesions.[14,46] Similarly, in our study we observed that *PD-L1* CN gains were more frequent in those specimens with PD-L1 expression. Thus, these results suggest that *PD-L1* genetic alterations may lead to PD-L1 upregulation in a subgroup of IVLBCL cases, as reported in other types of aggressive B-cell lymphoma,[7,48] indicating that immune evasion mechanisms are involved in the pathogenesis of IVLBCL. We have also identified mutations in other genes modulating the interaction of tumor cells with the microenvironment such as *CD58* and *B2M* in 3 (20%) cases. Interestingly, *TMEM30A* modulates phosphatidylserine residues in the cell membrane that may be recognized by macrophages. In an experimental murine model, *TMEM30A* truncating mutations promoted a macrophage-rich tumor microenvironment, and the tumors had an increased response to anti-CD47 checkpoint treatment promoting macrophages phagocytosis.[28] These observations and the relatively high frequency of *TMEM30A* mutations in IVLBCL may expand the perspectives of immunotherapy strategies in these tumors. Shimada et al[14] also found CNAs involving genes related to antigen presentation to T cells, such as *HLA-A*/*B*/*C* (33%) and *HLA* class II (9%). Altogether, these findings suggest that IVLBCL selects different types of oncogenic alterations promoting the immunosurveillance escape. The detection of PD-L1 expression and/or *PD-L1* CNAs in IVLBCL may help to identify patients who can benefit from programmed cell death protein 1/PD-L1 immune checkpoints inhibitors.

Our genomic analysis and programmed cell death protein 1/PD-L1 studies show similar results in classic and HPS-associated disease as well as in cases with and without extravascular extension suggesting that all these variants correspond to the same entity. Our study could not include primary cutaneous IVLBCL, which has been associated with a better outcome.[8] Future studies of the genomic alterations in these cases should determine whether they have a similar mutational profile.

In summary, our study expands the spectrum of pathologic features of IVLBCL, and confirms the genomic profile of these tumors characterized by frequent mutations in genes activating BCR/NF-κB pathway, particularly *PIM1*, *MYD88*^{L265P}, *CD79B*, *TMEM30A*, and *IRF4*, combined with aberrations in genes regulating immune escape, and identifies novel driver alterations (*IRF4* translocation, *NOTCH2*, *CCND3*, *GNA13*) in this uncommon lymphoma. These findings suggest the possible use of new target therapies and immune checkpoint inhibitors in the management of these patients.

ACKNOWLEDGMENTS

The authors thank Noelia Garcia, Silvia Martín, and Helena Suarez for their excellent technical assistance. They are indebted to the IDIBAPS Genomics Core Facility.

REFERENCES

1. Ponzoni M, Arrigoni G, Gould VE, et al. Lack of CD 29 (β1 integrin) and CD 54 (ICAM-1) adhesion molecules in intravascular lymphomatosis. *Hum Pathol*. 2000;31:220–226.
2. Fonkem E, Lok E, Robison D, et al. The natural history of intravascular lymphomatosis. *Cancer Med*. 2014;3:1010–1024.
3. Swerdlow SH, Campo E, Harris NL, et al. *WHO Classification of Tumours of Haematopoietic and Lymphoid Tissues*. International Agency for Research on Cancer; 2017.
4. Ponzoni MFAJ. Intravascular lymphoma: a neoplasm of "homeless" lymphocytes? *Hematol Oncol*. 2006;24:105–112.
5. Brunet V, Marouan S, Routy JP, et al. Retrospective study of intravascular large B-cell lymphoma cases diagnosed in Quebec. *Medicine*. 2017;96:1–8.
6. Shigematsu Y, Matsuura M, Nishimura N, et al. Intravascular large B-cell lymphoma of the bilateral ovaries and uterus in an asymptomatic patient with a t(11;22)(q23;q11) constitutional translocation. *Intern Med*. 2016;55:3169–3174.
7. Wang T, Ghaffar H, Grin A. Intravascular large B-cell lymphoma presenting with fulminant pseudomembranous colitis. *Pathol Res Pract*. 2013;209:323–326.

8. Ferreri AJM, Campo E, Seymour JF, et al. Intravascular lymphoma: clinical presentation, natural history, management and prognostic factors in a series of 38 cases, with special emphasis on the "cutaneous variant.". *Br J Haematol*. 2004;127:173–183.
9. Fujikura K, Yamashita D, Yoshida M, et al. Cytogenetic complexity and heterogeneity in intravascular lymphoma. *J Clin Pathol*. 2021;74:244–250.
10. Klairmont MM, Cheng J, Martin MG, et al. Recurrent cytogenetic abnormalities in intravascular large B-cell lymphoma. *Am J Clin Pathol*. 2018;150:18–26.
11. Shimada K, Shimada S, Sugimoto K, et al. Development and analysis of patient-derived xenograft mouse models in intravascular large B-cell lymphoma. *Leukemia*. 2016;30:1568–1579.
12. Schrader AMR, Jansen PM, Willemze R, et al. High prevalence of MYD88 and CD79B mutations in intravascular large B-cell lymphoma. *Blood*. 2018;131:2086–2089.
13. Suehara Y, Sakata-Yanagimoto M, Hattori K, et al. Liquid biopsy for the identification of intravascular large B-cell lymphoma. *Haematologica*. 2018;103:e241–e244.
14. Shimada K, Yoshida K, Suzuki Y, et al. Frequent genetic alterations in immune checkpoint–related genes in intravascular large B-cell lymphoma. *Blood*. 2021;137:1491–1502.
15. Kodgule R, Chen J, Khonde P, et al. Recurrent Switch 2 domain RAC2 mutations in intravascular large B-cell lymphoma. *Blood Adv*. 2022;[Epub ahead of print].
16. Shimada K, Kinoshita T, Naoe T, et al. Presentation and management of intravascular large B-cell lymphoma. *Lancet Oncol*. 2009; 10:895–902.
17. Henter J-I, Horne A, Aricó M, et al. HLH-2004: diagnostic and therapeutic guidelines for hemophagocytic lymphohistiocytosis. *Pediatr Blood Cancer*. 2007;48:124–131.
18. Johnson NA, Slack GW, Savage KJ, et al. Concurrent expression of MYC and BCL2 in diffuse large B-cell lymphoma treated with rituximab plus cyclophosphamide, doxorubicin, vincristine, and prednisone. *J Clin Oncol*. 2012;30:3452–3459.
19. Hans CP, Weisenburger DD, Greiner TC, et al. Confirmation of the molecular classification of diffuse large B-cell lymphoma by immunohistochemistry using a tissue microarray. *Blood*. 2004;103:275–282.
20. Huang S, Nong L, Liang L, et al. Comparison of PD-L1 detection assays and corresponding significance in evaluation of diffuse large B-cell lymphoma. *Cancer Med*. 2019;8:3831–3845.
21. Fang X, Xiu B, Yang Z, et al. The expression and clinical relevance of PD-1, PD-L1, and TP63 in patients with diffuse large B-cell lymphoma. *Medicine*. 2017;96:e6398.
22. Salaverria I, Philipp C, Oschlies I, et al. Translocations activating IRF4 identify a subtype of germinal center-derived B-cell lymphoma affecting predominantly children and young adults. *Blood*. 2011;118: 139–147.
23. Veloza L, Teixido C, Castrejon N, et al. Clinicopathological evaluation of the programmed cell death 1 (PD1)/programmed cell death-ligand 1 (PD-L1) axis in post-transplant lymphoproliferative disorders: association with Epstein–Barr virus, PD-L1 copy number alterations, and outcome. *Histopathology*. 2019;75:799–812.
24. Roemer MGM, Advani RH, Ligon AH, et al. PD-L1 and PD-L2 genetic alterations define classical hodgkin lymphoma and predict outcome. *J Clin Oncol*. 2016;34:2690–2697.
25. Rivas-Delgado A, Nadeu F, Enjuanes A, et al. Mutational landscape and tumor burden assessed by cell-free DNA in diffuse large B-cell lymphoma in a population-based study. *Clin Cancer Res*. 2021;27:513–521.
26. Ramis-Zaldivar JE, Gonzalez-Farre B, Balague O, et al. Distinct molecular profile of IRF4-rearranged large B-cell lymphoma. *Blood*. 2020;135:274–286.
27. Frauenfeld L, Castrejon-de-Anta N, Ramis-Zaldivar JE, et al. Diffuse large B-cell lymphomas in adults with aberrant coexpression of CD10, BCL6, and MUM1 are enriched in IRF4 rearrangements. *Blood Adv*. 2022;6:2361–2372.
28. Ennishi D, Healy S, Bashashati A, et al. TMEM30A loss-of-function mutations drive lymphomagenesis and confer therapeutically exploitable vulnerability in B-cell lymphoma. *Nat Med*. 2020;26:577–588.
29. Kiriakopoulos A, Linos D. Intravascular B-large cell lymphoma: an unexpected diagnosis of an incidental adrenal mass. *J Surg Case Rep*. 2019;2019:1–3.
30. Ho CWG, Mantoo S, Lim CH, et al. Synchronous invasive ductal carcinoma and intravascular large B-cell lymphoma of the breast: a case report and review of the literature. *World J Surg Oncol*. 2014;12:88.
31. Wang BY, Strauchen JA, Rabinowitz D, et al. Renal cell carcinoma with intravascular lymphomatosis: a case report of unusual collision tumors with review of the literature. *Arch Pathol Lab Med*. 2001; 125:1239–1241.
32. Satoh T, Arai E, Kayano H, et al. Pulmonary intravascular large B-cell lymphoma accompanying synchronous primary pulmonary adenocarcinoma and benign interstitial lesions. *J Clin Exp Hematopathol*. 2019;59:140–144.
33. Cheng CL, Su YC, Chao TY, et al. Intralymphatic spread is a rare finding associated with poor prognosis in diffuse large B-cell lymphoma with extranodal involvements. *Am J Surg Pathol*. 2018;42:616–624.
34. Itami H, Nakamine H, Kubo M, et al. Diffuse large B-cell lymphoma (DLBCL) with significant intravascular invasion. Close resemblance of its clinicopathological features to intravascular large B-cell lymphoma, but not to DLBCL-not otherwise specified. *J Clin Exp Hematopathol*. 2021;61:152–161.
35. Chapuy B, Stewart C, Dunford A, et al. Molecular subtypes of diffuse large B-cell Lymphoma are associated with distinct pathogenic mechanisms and outcomes. *Nat Med*. 2018;24:679–690.
36. Schmitz R, Wright GW, Huang DW, et al. Genetics and pathogenesis of diffuse large B-cell lymphoma. *N Engl J Med*. 2018;378:1396–1407.
37. Wright GW, Huang DW, Phelan JD, et al. A probabilistic classification tool for genetic subtypes of diffuse large B cell lymphoma with therapeutic implications. *Cancer Cell*. 2020;37:551. e14–568.e14.
38. Campo E, Jaffe ES, Cook JR, et al. The International Consensus Classification of Mature Lymphoid Neoplasms: a report from the Clinical Advisory Committee. *Blood*. 2022;140:1229–1253.
39. Szydłowski M, Prochorec-Sobieszek M, Szumera-Ciećkiewicz A, et al. Expression of PIM kinases in Reed-Sternberg cells fosters immune privilege and tumor cell survival in Hodgkin lymphoma. *Blood*. 2017;130:1418–1429.
40. Szydłowski M, Dębek S, Prochorec-Sobieszek M, et al. PIM kinases promote survival and immune escape in primary mediastinal large B-cell lymphoma through modulation of JAK-STAT and NF-κB activity. *Am J Pathol*. 2021;191:567–574.
41. Ngo VN, Young RM, Schmitz R, et al. Oncogenically active MYD88 mutations in human lymphoma. *Nature*. 2011;470:115–119.
42. Davis RE, Ngo VN, Lenz G, et al. Chronic active B-cell-receptor signalling in diffuse large B-cell lymphoma. *Nature*. 2010;463:88–92.
43. Karube K, Enjuanes A, Dlouhy I, et al. Integrating genomic alterations in diffuse large B-cell lymphoma identifies new relevant pathways and potential therapeutic targets. *Leukemia*. 2018;32:675–684.
44. Schmitz R, Young RM, Ceribelli M, et al. Burkitt lymphoma pathogenesis and therapeutic targets from structural and functional genomics. *Nature*. 2012;490:116–120.
45. Gupta GK, Jaffe ES, Pittaluga S. A study of PD-L1 expression in intravascular large B-cell lymphoma: correlation with clinical and pathologic features. *Histopathology*. 2019;75:282–286.
46. Patel N, Slack GW, Bodo J, et al. Immune escape mechanisms in intravascular large B-cell lymphoma: a molecular cytogenetic and immunohistochemical study. *Am J Clin Pathol*. 2022;157:578–585.
47. Suzuki Y, Kohno K, Matsue K, et al. PD-L1 (SP142) expression in neoplastic cells predicts a poor prognosis for patients with intravascular large B-cell lymphoma treated with rituximab-based multiagent chemotherapy. *Cancer Med*. 2020;9:4768–4776.
48. Green MR, Monti S, Rodig SJ, et al. Integrative analysis reveals selective 9p24.1 amplification, increased PD-1 ligand expression, and further induction via JAK2 in nodular sclerosing Hodgkin lymphoma and primary mediastinal large B-cell lymphoma. *Blood*. 2010;116:3268–3277.

